

Graphene electrons beyond the linear dispersion regime

S. R. Power and M. S. Ferreira*

School of Physics, Trinity College Dublin, Dublin 2, Ireland

(Dated: January 26, 2023)

Among the many interesting features displayed by graphene, one of the most attractive is the simplicity with which its electronic structure can be described. The study of its physical properties is significantly simplified by the linear dispersion relation of electrons in a narrow range around the Fermi level. Unfortunately, the mathematical simplicity of graphene electrons is only limited to this narrow energy region and is useless when dealing with problems that involve energies outside the linear dispersion part of the spectrum. In this letter we remedy this limitation by deriving a set of closed-form analytical expressions for the real-space single-electron Green function of graphene which are valid across an enormous fraction of the energy spectrum. By extending to a wider energy range the simplicity with which graphene electrons are described, it is now possible to derive more mathematically transparent and insightful expressions for a number of physical properties that involve higher energy scales. The power of this new formalism is illustrated in the case of the magnetic (RKKY) interaction in graphene.

PACS numbers:

Graphene-related materials have been in the scientific limelight for the past few years due to the numerous applications envisaged for them[1]. Besides the huge potential for applicability, one key feature that makes graphene particularly popular is the simplicity with which many of its physical properties can be described, primarily due to the simple dispersion relation for its electrons. The linearity of this dispersion relation around the Fermi level enables the description of graphene electrons in terms of massless Dirac fermions[2]. This introduces a great level of mathematical transparency in the portrayal of their properties, which nevertheless is limited only to a narrow range of energies around the Fermi level. Energy values outside this range are often needed but lack the mathematical transparency of those within the linear dispersion regime. In this letter we show how this limitation can be circumvented by deriving a fully analytical closed-form expression for the single-electron Green function of graphene in real space, a quantity that is instrumental in describing the behaviour of graphene electrons. Because Green functions are used in the study of several physical properties, improvements in their mathematical description will enable far more transparent and insightful expressions for the corresponding physical quantities. This is illustrated for the case of the magnetic interaction in graphene, where a fully analytical method is used to derive the principal features of the interaction.

The general formula for the single-electron Green function, within the nearest-neighbour tight-binding framework, in its eigenstate basis is

$$\hat{G}(E) = \sum_{\vec{k}} \left\{ \frac{|\vec{k}, +\rangle\langle\vec{k}, +|}{E - \mathcal{E}_+(\vec{k})} + \frac{|\vec{k}, -\rangle\langle\vec{k}, -|}{E - \mathcal{E}_-(\vec{k})} \right\}, \quad (1)$$

where E is the energy, $|\vec{k}, \pm\rangle$ is the eigenvector labeled by

the wave vector \vec{k} and \mathcal{E}_{\pm} is the corresponding eigenvalue defined as

$$\mathcal{E}_{\pm}(\vec{k}) = \pm t \sqrt{1 + 4 \cos\left(\frac{\sqrt{3}k_y a}{2}\right) \cos\left(k_x \frac{a}{2}\right) + 4 \cos^2\left(k_x \frac{a}{2}\right)}. \quad (2)$$

The quantities a and t correspond to the lattice parameter of graphene and its nearest-neighbour electronic hopping, respectively, which are hereafter used as our units of distance and energy. Our choice is such that the x (y) direction is aligned to the zigzag (armchair) geometry of the graphene lattice. A simple unitary transformation defines the real-space basis $|j, \zeta\rangle$, where the index j labels the two-atom unit cell and the index ζ refers to the intra-cell atoms corresponding to the two distinct sublattices of graphene. When projected onto two different states $|j, \zeta\rangle$ and $|j', \zeta'\rangle$ located in real space by the respective vectors \vec{R}_j and $\vec{R}_{j'}$, the Green function is written as

$$\langle j, \zeta | \hat{G}(E) | j', \zeta' \rangle = \frac{a^2 \sqrt{3}}{8\pi^2} \int_{-\frac{\pi}{a}}^{\frac{\pi}{a}} dk_x \int_{\frac{-2\pi}{a\sqrt{3}}}^{\frac{-2\pi}{a\sqrt{3}}} dk_y \frac{E e^{i\vec{k} \cdot (\vec{R}_j - \vec{R}_{j'})}}{E^2 - \mathcal{E}_{\pm}^2(\vec{k})}. \quad (3)$$

Although we have selected two states that belong to the same sublattice ($\zeta = \zeta'$), this constraint can be easily relaxed and generalized to describe the propagator between sites on different sublattices. Before showing how to solve the integrals that appear in Eq.(3), we will outline the basic steps taken to obtain the Green function. We tackle the first integral by analytical continuation to the complex plane, where it is subsequently solved using the residue theorem.[3, 4] The remaining integral can then be solved in the case of moderately large separation vectors by using the stationary phase approximation.[5]

For the sake of simplicity we consider the separation vectors $\vec{R}_j - \vec{R}_{j'}$ along the (armchair) y -direction. This is by no means the only case in which our method works, but it is a case in which the solutions are very transparent. By showing how to obtain the Green function for

*Electronic address: ferreirm@tcd.ie

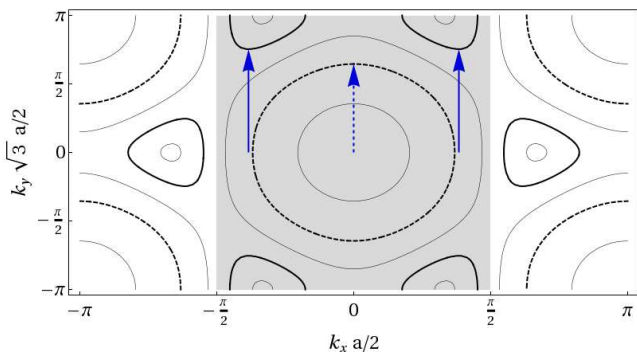


FIG. 1: Constant energy plots of the function $\mathcal{E}_+(\vec{k})$ in reciprocal space for a few different energies. Horizontal and vertical axes are rescaled as $k_x a/2$ and $k_y a\sqrt{3}/2$, respectively, so that they are plotted as dimensionless quantities. The rectangular shaded area delimits the first Brillouin zone over which the integrals in Eq.(3) are taken. Constant energy plots for two specific energies, $E = 0.7t$ (solid) and $E = 1.8t$ (dashed), are drawn with thicker lines. The corresponding stationary wave vectors \vec{q} for these energies are highlighted with arrows. Note that the sign of \vec{q} , shown as positive here for simplicity, must be chosen according to the conditions outlined in the text.

this particular case we hope to illustrate how the solution for separation vectors along arbitrary directions can be obtained. Note that the position vectors appear only as a difference and can be further simplified by defining $\Delta \equiv |\vec{R}_j - \vec{R}_{j'}|$. In this case, the integral above can be evaluated by extending k_y to the realm of complex numbers and changing the integration contour from a straight line on the real axis to the boundaries of a semi-infinite rectangle in the upper half of the complex plane, with its base lying on the real axis between $-\frac{2\pi}{a\sqrt{3}}$ and $\frac{2\pi}{a\sqrt{3}}$. Because the integrand vanishes in the limit $\text{Im}[k_y] \rightarrow \infty$ and because the parts of the contour that are parallel to the imaginary axis cancel each other out, the k_y -integral can be evaluated by simply identifying the poles of the integrand lying inside the integration contour and finding their respective residues [3], that is,

$$\mathcal{G}_\Delta(E) = \frac{ia}{4\pi t^2} \int_{-\pi/a}^{\pi/a} dk_x \frac{E e^{iq\Delta}}{\cos(\frac{k_x a}{2}) \sin(\frac{qa\sqrt{3}}{2})}. \quad (4)$$

Note that the scalar product $\langle j, \zeta | \hat{\mathcal{G}}(E) | j', \zeta' \rangle$ is now more concisely expressed as $\mathcal{G}_\Delta(E)$ and that

$$\cos\left(\frac{qa\sqrt{3}}{2}\right) = \frac{\frac{E^2}{t^2} - 1 - 4\cos^2\left(\frac{k_x a}{2}\right)}{4\cos\left(\frac{k_x a}{2}\right)} \quad (5)$$

defines the wave vector q that comes out of the first integral. Although Eq.(5) provides a unique definition for $\cos\left(\frac{qa\sqrt{3}}{2}\right)$, it does not specify the sign of q uniquely. Its sign is selected by imposing that q must necessarily lie within the integration contour of the k_y -integral.

The k_x -dependence contained in the wave vector q , as seen in Eq.(5), means that the integrand in Eq. (4) is

an oscillatory function of k_x that oscillates very rapidly for large values of the separation Δ . In this case, the only non-vanishing contribution to the Green function comes from regions for which the phase of the exponential function is stationary. To locate these stationary points we must impose that $dq/dk_x = 0$, which leads to solutions of the form

$$\tilde{k}_x = \begin{cases} \pm \frac{2}{a} \cos^{-1}\left(\frac{\sqrt{t^2 - E^2}}{2t}\right) & \text{if } |E| < t \\ 0 & \text{if } |E| > t \end{cases} \quad (6)$$

Note that due to a topological change in the constant energy surfaces of the function $\mathcal{E}_+(\vec{k})$ at $E = \pm t$ we separate the energy band into two separate regions, namely, the inner region defined by $|E| < |t|$ and the outer region defined by $|E| > |t|$. Both stationary solutions written above are valid throughout the entire energy spectrum. However, outside those specified regions, albeit solutions, they give rise to complex values for the wave vectors q . With complex wave vectors, the integrand of Eq.(4) tends to vanish for any sizable separation Δ , meaning that the stationary values outside the ranges listed in Eq.(3) should have very little influence in the overall results for the Green functions.[6] The same can be understood from purely geometrical arguments applied to the constant energy surfaces of $\mathcal{E}_+(\vec{k})$ in reciprocal space, depicted in Fig. 1. When searching for stationary solutions for q , which in this case lie parallel to the y -axis, the two solutions resulting from Eq.(6) are the only possible (real) ones within the rectangular Brillouin zone of the hexagonal lattice. The tilde symbol (\sim) will hereafter be used to refer to the values of k_x and q satisfying the stationary condition. Therefore, the wave vector q when expanded in a Taylor series around the stationary value \tilde{k}_x has no linear component and, up to second order, is approximated by

$$q \approx C_1 + C_2 (k_x - \tilde{k}_x)^2, \quad (7)$$

where

$$C_1 = \frac{2}{a\sqrt{3}} \cos^{-1}\left(\frac{-\sqrt{t^2 - E^2}}{t}\right) \quad (8)$$

and

$$C_2 = \frac{a}{4\sqrt{3}} \left(\frac{E^2 + 3t^2}{E\sqrt{t^2 - E^2}}\right). \quad (9)$$

Note that the sign of C_1 must be chosen to ensure that q lies within the k_y integration contour as before. The sign of C_2 is determined by its correspondence to the curvature of q at \tilde{k}_x . If we now insert Eq.(7) into Eq.(4) and make use of the fact that k_x and q will not vary very much around their respective stationary values \tilde{k}_x and \tilde{q} , we are left with a much simplified expression for the Green function, which now reads

$$\mathcal{G}_\Delta(E) = \frac{iaE e^{iC_1\Delta}}{4\pi t^2 \cos\left(\frac{\tilde{k}_x a}{2}\right) \sin\left(\frac{\tilde{q} a\sqrt{3}}{2}\right)} \int dk_x e^{iC_2(k_x - \tilde{k}_x)^2 \Delta}. \quad (10)$$

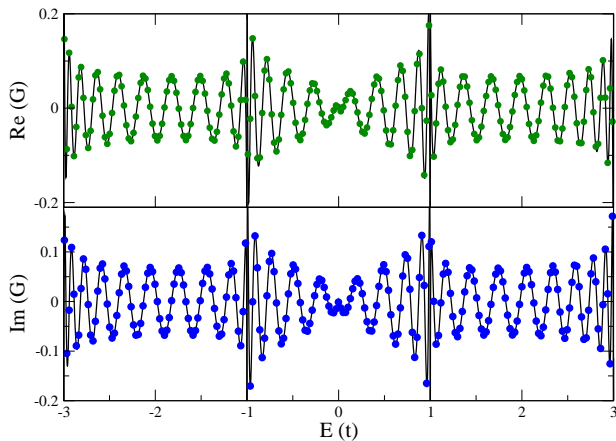


FIG. 2: $\mathcal{G}_\Delta(E)$ as a function of energy (in units of t) for the case of $\Delta = 10\sqrt{3}a$. Top (Bottom) panel shows the real (imaginary) part of the Green function. Lines correspond to the results evaluated by Eq.(11) whereas points are the result of brute-force numerical calculations of Eq.(3).

The remaining integral is a well known Gaussian integral whose solution gives

$$\mathcal{G}_\Delta(E) = \frac{iaEe^{iC_1\Delta}}{4\pi t^2 \cos\left(\frac{\tilde{k}_x a}{2}\right) \sin\left(\frac{\tilde{q} a \sqrt{3}}{2}\right)} \sqrt{\frac{i\pi}{C_2 \Delta}}. \quad (11)$$

Eq.(11) together with the definitions in Eqs. (5), (6), (8) and (9) provide the complete expression for the off-diagonal Green function matrix element between two graphene sites separated by a distance Δ along the armchair direction. Fig. 2 compares both the real and imaginary parts of the Green function for the case of $\Delta = 10\sqrt{3}a$ obtained by the analytical expression above with those obtained through a numerical evaluation of Eq.(3).

At first glance one might think that the replacement of the well established linear dispersion approximation with another that is valid only for asymptotically large values of separation is unlikely to improve the range of validity of the overall result. However, as seen in Fig. 2, there is hardly any noticeable difference between the analytical and numerical results across the entire energy band. Because the analytical expression relies on the stationary phase argument, this remarkable agreement is likely to regress as the separation (Δ) is reduced. To test how good an approximation Eq.(11) is, in Fig. 3 we plot the fraction $\mathcal{F}_{1\%}$ of the bandwidth for which the relative error between the numerical and analytical evaluations is less than 1% as a function of the separation. Even for small separations ($\Delta \approx 10a$), the energy range for which the Green functions are very accurately described by our analytical expression exceeds 90% of the bandwidth. In other words, there is only a very narrow energy range in which the disagreement exceeds 1%. Most remarkably, as the separation is increased this small range decreases very rapidly, indicating that Eq.(11) is capable of accurately

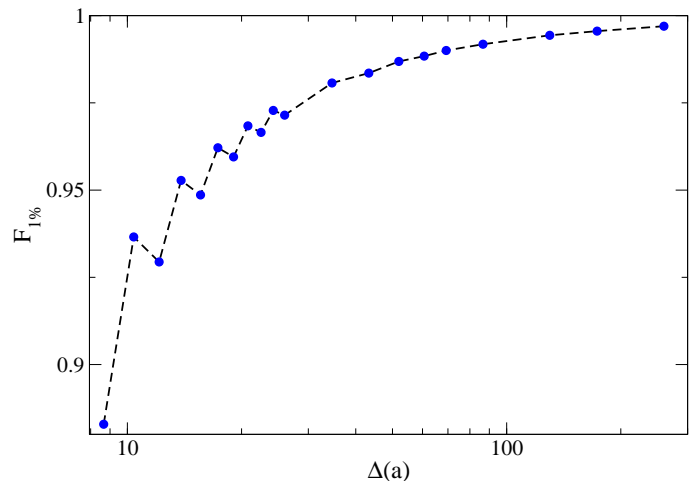


FIG. 3: Fraction $\mathcal{F}_{1\%}$ of the bandwidth for which the error between the analytical and brute force numerical results is below 1%, plotted as a function of the separation Δ (in units of a).

describing the Green function across almost the entire energy spectrum for separation values larger than a few lattice parameters. This is undoubtedly a major advance when compared to the narrow fraction of the bandwidth that meets the linear dispersion criterion.

Having presented the derivation of the Green function for the separation vector along the armchair direction, it is straightforward to generalize it to other cases. For separation vectors parallel to the zigzag direction the method followed is identical. For arbitrary directions, or Green functions between sites on opposite sublattices, the procedure is similar, however the identification of stationary solutions may occasionally result from high order polynomial equations that are not always analytically solvable. But even in these cases, there are special directions for which the solutions are simply obtained.

The usefulness of having an analytical expression for the real space Green function, valid throughout the entire electronic energy band, becomes obvious when physical properties of graphene involving energy scales outside the linear dispersion region are investigated. This is particularly advantageous when such properties carry size or position dependence because in this case Eq.(11) can be more concisely expressed as

$$\mathcal{G}_\Delta(E) = \frac{\mathcal{A}(E) e^{iC_1(E)\Delta}}{\sqrt{\Delta}}, \quad (12)$$

so that the E - and Δ -dependences are clearly distinguished. Furthermore, even in the case when the functional form of the coefficient $\mathcal{A}(E)$ is not particularly simple, the expression in Eq.(11) can be used to expand the Green function in a polynomial series, which is undoubtedly far simpler and more treatable than the original expression in Eq.(3). The ability to clearly isolate the distance dependent part of the Green function will

allow a more transparent treatment of some of the more eagerly investigated properties of graphene.

To demonstrate the power and applicability of our new formalism, we turn our attention to the exchange interaction in graphene. This interaction determines the relative orientation of magnetic moments embedded in graphene and has been the subject of many recent papers[7–13], as an understanding of this interaction is a major step in the implementation of graphene devices in the field of spintronics. When the linear dispersion approximation is used, a cut-off function is required to prevent the result diverging due to high energy contributions. There has been some debate about the effect of the cutoff function chosen on the resultant interaction calculated[7, 8, 11]. Other approaches to circumvent this problem involve numerical calculations[11, 13] which can lack the transparency of an analytical solution. Here we shall show that the decay rate and oscillation period of the interaction as a function of distance emerge naturally from a simple calculation using our formalism and without resorting to an energy cut-off or a restriction to the linear dispersion regime. The exchange energy, J , within the RKKY approximation[14–16] is proportional to the static susceptibility, χ , which can in turn be written in terms of Green functions, allowing us to write $J_\Delta(E_F) \sim \text{Im} \int dE f(E) \mathcal{G}_\Delta^2(E)$ for two moments occupying like-sites in the graphene lattice separated by a distance Δ . This quantity relates to the energy difference between the ferromagnetic and antiferromagnetic alignment of the moments, with its sign giving the energetically favourable alignment. Using the expression in Eq. (12) we write

$$J_\Delta \sim \text{Im} \int dE \frac{\mathcal{B}(E) e^{2iC_1(E)\Delta}}{\Delta(1 + e^{\beta(E-E_F)})}, \quad (13)$$

where $\mathcal{B}(E) = \mathcal{A}^2(E)$, $\beta = \frac{1}{k_B T}$, T being the temperature and k_B the Boltzmann constant. The integral in Eq (13) can be solved by replacing it with a contour integral in the energy upper-half plane. In this case the poles are given by the zeroes of the denominator of the Fermi function, namely the Matsubara frequencies, $E_p = E_F + i(2p+1)\pi k_B T$ where p is an integer labelling the poles. Writing the coefficient $\mathcal{B}(E)$ as a Taylor series, and the wavevector $C_1(E)$ as a first order expansion, around the Fermi energy gives

$$J_\Delta \sim \frac{k_B T}{\Delta} \sum_l \frac{1}{l!} \mathcal{B}^{(l)} e^{2iC_1^{(0)}\Delta} \sum_p e^{2iC_1^{(1)}(E_p-E_F)\Delta} (E_p-E_F)^l, \quad (14)$$

using $\mathcal{B}^{(l)}$ ($C_1^{(l)}$) to denote the l th derivative of \mathcal{B} (C_1) evaluated at the Fermi energy. This can be rewritten as

$$J_\Delta \sim \frac{1}{\Delta} \sum_l \frac{1}{l!} \mathcal{B}^{(l)} \frac{e^{2iC_1^{(0)}\Delta}}{(2iC_1^{(1)})^l} \frac{d^l}{d\Delta^l} \left\{ \frac{k_B T}{2\sinh(2C_1^{(1)}\pi k_B T \Delta)} \right\}. \quad (15)$$

In the low temperature limit, $T \rightarrow 0$, this expression

simplifies to one of the form

$$J_\Delta(E_F) \sim \sum_l \mathcal{B}^{(l)}(E_F) \frac{e^{2iC_1(E_F)\Delta}}{\Delta^{l+2}}. \quad (16)$$

In this form the oscillation period and decay rate of the interaction at different Fermi energies can be easily extracted. The decay rate in the asymptotic limit is determined by the leading term in Eq (16), namely $l = 0$, suggesting that, in general, $J \sim \Delta^{-2}$. However, at $E_F = 0$, it is straightforward to see from the analytical expression that the coefficient $\mathcal{B}^{(0)}$ vanishes and the decay rate is in fact determined by the first surviving term, $l = 1$, resulting in $J \sim \Delta^{-3}$ for undoped graphene, as reported elsewhere in the literature[7, 8, 11, 13]. Also, at $E_F = 0$, the oscillation period is perfectly commensurate with the graphene lattice spacing and thus oscillations are masked. When $E_F \neq 0$, the leading term does not vanish, and the oscillation period is no longer commensurate with the lattice spacing, leading to the observed oscillatory interaction[8] that decays as $J \sim \Delta^{-2}$. Note that these conclusions are reached for values of E_F regardless of whether they lie within the linear dispersion regime. The correct decay rate and oscillatory behaviour for the RKKY interaction in graphene have emerged naturally and in a mathematically transparent fashion from our formalism, without resort to the linear response approximation or the need for a cut-off function. As far as the authors are aware, this is the first time this has been performed within a fully analytical framework.

Studies of other features in graphene, such as Friedel oscillations[17], and indeed, general disorder properties[18], are usually undertaken within the Green function framework, but often only in the linear dispersion regime. The approach described here for the magnetic interaction can be modified straightforwardly to extend the validity of expressions derived in such studies beyond this regime. Because so many physical quantities are dependent on the single-particle Green functions, the understanding of graphene previously allowed by its linear dispersion simplicity can now be extended and enhanced. In summary, we have derived a closed-form expression for the single-electron Green function of graphene in real space that does not rely on the linearity of its dispersion relation near the Fermi level. The expression is valid across a very large fraction of the energy band and yet remains mathematically transparent. This newly-acquired simplicity with which we can describe the electronic properties of graphene will serve as a reference to others investigating the physical properties of graphene and will lead to insightful new ways of studying graphene in energy scales well beyond the linear dispersion regime, as we have shown here for the RKKY interaction in graphene.

Acknowledgments

The authors wish to acknowledge support received from Science Foundation Ireland and the Irish Research Council for Science, Engineering and Technology under

the EMBARK initiative. MSF thanks A. H. Castro Neto, V. M. Pereira and M. D. Barrozo for fruitful discussions during his stay in Boston and the Condensed Matter Theory Visitor's Program at Boston University for support.

-
- [1] A. K. Geim and K. S. Novoselov, *Nature Materials*, **6**, 183 (2007)
 - [2] A. H. Castro Neto, F. Guinea, N. M. R. Peres, K. S. Novoselov and A. K. Geim, *Rev. Mod. Phys.* **81**, 109 (2009)
 - [3] A. T. Costa, D. F. Kirwan and M. S. Ferreira, *Phys. Rev. B* **72**, 085402 (2005)
 - [4] M. L. Boas, *Mathematical Methods in the Physical Sciences*, Wiley (1983)
 - [5] A. A. Abrikosov, *Fundamentals of the Theory of Metals*, North Holland (1988)
 - [6] Accounting for both stationary solutions improve the result only for energies very near the van Hove singularities at $E = \pm t$. Other than that, the excluding conditions at Eq.(6) are sufficient.
 - [7] S. Saremi, *Phys. Rev. B* **76**, 184430 (2007)
 - [8] L. Brey, H. A. Fertig and S. Das Sarma, *Phys. Rev. Lett.* **99**, 116802 (2007)
 - [9] M. A. H. Vozmediano, M. P. Lopez-Sancho, T. Stauber and F. Guinea, *Phys. Rev. B* **72**, 155121 (2005)
 - [10] V. K. Dugaev, V. I. Litvinov and J. Barnas, *Phys. Rev. B* **74**, 224438 (2006)
 - [11] A. M. Black-Schaffer, *Phys. Rev. B* **81**, 205416 (2010)
 - [12] J. E. Bunder and H. H. Lin, *Phys. Rev. B* **80**, 153414 (2009)
 - [13] M. Sherafati and S. Satpathy, arXiv:1008.4834 (unpublished)
 - [14] M. A. Ruderman and C. Kittel, *Phys. Rev.* **96**, 99 (1954)
 - [15] T. A. Kasuya, *Prog. Theor. Phys.* **16**, 45 (1956)
 - [16] K. Yosida, *Phys. Rev.* **106**, 893 (1957)
 - [17] C. Bena, *Phys. Rev. Lett.* **100**, 076601 (2008)
 - [18] V. M. Pereira, J. M. B. Lopes dos Santos and A. H. Castro Neto, *Phys. Rev. B* **77**, 115109 (2008)